ORIGINAL ARTICLE

Cerebral cortex involvement in Machado–Joseph disease

T. J. R. de Rezende[a,b], A. D'Abreu[a], R. P. Guimarães[a], T. M. Lopes[a], I. Lopes-Cendes[c], F. Cendes[a], G. Castellano[b] and M. C. França Jr[a]

[a]*Department of Neurology, University of Campinas (UNICAMP), Campinas;* [b]*Department of Cosmic Rays and Chronology, University of Campinas (UNICAMP), Campinas; and* [c]*Department of Medical Genetics, University of Campinas (UNICAMP), Campinas, Brazil*

Keywords:
cerebral cortex, cortical thickness, FreeSurfer, Machado–Joseph disease, neuropsychological tests

Received 13 March 2014
Accepted 25 July 2014

European Journal of Neurology 2015, **22:** 277–283

doi:10.1111/ene.12559

Background and purpose: Machado–Joseph disease (MJD/SCA3) is the most frequent spinocerebellar ataxia, characterized by brainstem, basal ganglia and cerebellar damage. Few magnetic resonance imaging based studies have investigated damage in the cerebral cortex. The objective was to determine whether patients with MJD/SCA3 have cerebral cortex atrophy, to identify regions more susceptible to damage and to look for the clinical and neuropsychological correlates of such lesions.

Methods: Forty-nine patients with MJD/SCA3 (mean age 47.7 ± 13.0 years, 27 men) and 49 matched healthy controls were enrolled. All subjects underwent magnetic resonance imaging scans in a 3 T device, and three-dimensional T1 images were used for volumetric analyses. Measurement of cortical thickness and volume was performed using the FreeSurfer software. Groups were compared using ANCOVA with age, gender and estimated intracranial volume as covariates, and a general linear model was used to assess correlations between atrophy and clinical variables.

Results: Mean CAG expansion, Scale for Assessment and Rating of Ataxia (SARA) score and age at onset were 72.1 ± 4.2, 14.7 ± 7.3 and 37.5 ± 12.5 years, respectively. The main findings were (i) bilateral paracentral cortex atrophy, as well as the caudal middle frontal gyrus, superior and transverse temporal gyri, and lateral occipital cortex in the left hemisphere and supramarginal gyrus in the right hemisphere; (ii) volumetric reduction of basal ganglia and hippocampi; (iii) a significant correlation between SARA and brainstem and precentral gyrus atrophy. Furthermore, some of the affected cortical regions showed significant correlations with neuropsychological data.

Conclusions: Patients with MJD/SCA3 have widespread cortical and subcortical atrophy. These structural findings correlate with clinical manifestations of the disease, which support the concept that cognitive/motor impairment and cerebral damage are related in disease.

Introduction

Machado–Joseph disease (MJD/SCA3) is the most frequent autosomal dominant spinocerebellar ataxia worldwide. It is a neurodegenerative disease characterized by remarkable phenotypic heterogeneity and caused by an unstable mutation (CAG repeat expansion) at the *ATXN3* (*MJD1*) gene on chromosome 14q. The clinical manifestations include ataxia, peripheral neuropathy, ophthalmoparesis, pyramidal symptoms, dystonia, sleep disorders or parkinsonism. Furthermore, it is known that CAG repeat length correlates with age at onset and disease severity [1].

Neuroimaging studies have been very valuable in characterizing brain damage in spinocerebellar ataxias

Correspondence: M. C. França Jr, MD, PhD, Department of Neurology, University of Campinas – UNICAMP, Rua Tessália Vieira de Camargo, 126, Cidade Universitaria 'Zeferino Vaz', Campinas, SP 13083-887, Brazil (tel.: +55 19 3521 9217; fax: +55 19 351 7933; e-mail: mcfrancajr@uol.com.br).

(SCAs) and MJD/SCA3 in particular. In MJD/SCA3, however, some of these magnetic resonance imaging (MRI) based studies relied solely upon visual analysis or manual quantification [2]. In fact, only a few have used automated volumetric measurements [2–4]. Furthermore, most neuroimaging reports have focused on the cerebellum and its direct connections, such as brainstem, spinal cord and basal ganglia, because ataxia is the major clinical characteristic in the disease [1,5] Interestingly, little is known about cerebral cortical damage in these patients [6]. D'Abreu *et al.* [7] employed a voxel-based morphometry (VBM) approach in a large cohort of patients and found atrophy in the neocortex, including frontal, parietal, temporal and occipital lobes. Furthermore, some studies using positron emission tomography (PET) and single photon emission tomography (SPECT) showed involvement of the cortex in this illness [8].

These imaging data strongly suggest that neurodegeneration in MJD/SCA3 extends far beyond the cerebellum and motor pathways. In the last few years, cognitive deficits have been increasingly recognized in the disease. Lopes *et al.* [9] found episodic and working memory deficits, whereas Kawai *et al.* [10] also identified difficulties in visuospatial and language tasks. Such neuropsychological abnormalities cannot be explained exclusively by cerebellar damage. In this scenario, it is crucial to systematically investigate cerebral cortex damage in patients with MJD/SCA3 and to determine whether it correlates with neuropsychological findings. Recent advances in MRI analyses now enable reliable investigation of cerebral cortex damage, using tools such as the FreeSurfer package (http://surfer.nmr.mgh.harvard.edu). FreeSurfer performs automatic segmentation of all cortical and subcortical structures in the brain, thus enabling determination of the volume, area and thickness of the cerebral cortex. Measurements are accurate and present high reproducibility [11]. This methodology has been successfully used in other neurodegenerative disorders. Therefore, the primary aim of this study was to determine whether patients with MJD/SCA3 have cerebral cortex atrophy and to identify regions more susceptible to damage. As a secondary objective, clinical correlates of such involvement were investigated including both motor and cognitive functioning.

Materials

Participants

This study was approved by our institution research ethics committee and written signed consent was obtained from all subjects. Forty-nine adult symptomatic patients (27 men) with molecular confirmation of MJD/SCA3 and 49 healthy controls (27 men) were enrolled in the study (Table 1). All patients were recruited from the neurology and neurogenetics outpatient clinics (Department of Neurology, University of Campinas, Campinas, Brazil) between 2009 and 2013. Patients with unavailable clinical or genetic data were excluded from the study.

Neurological and cognitive evaluation

For each patient, information about age at onset, disease duration and CAG repeat length were recorded. In addition, a neurologist performed the Scale for Assessment and Rating of Ataxia (SARA) [12] on the same day as the MRI acquisition.

A subgroup of 28 patients also underwent neuropsychological assessment, performed by a trained psychologist [9]. Mean age and educational level of these subjects were 46.5 ± 11.5 years and 10.0 ± 4.0 years, respectively. The following tests, validated for the Portuguese language, were included: Rey auditory verbal learning test (coding, delayed recall and recognition); Corsi block-tapping task (forward and backward); digits span – forward and backward; semantic verbal fluency (animal category); figure memory, logical memory I and II and associated paired visual I and II subtests (WMS-R); similarities and picture completion (WAIS III subtest); Boston naming test; Hooper visual organization; Wisconsin card sorting test; and Raven Progressive Matrix Test (General Scale). Beck inventories for depression (BDI) and anxiety (BAI) were also applied to these 28 patients to evaluate depressive symptoms and anxiety. Mean BAI, BDI and educational level scores in this subgroup were 10.0 ± 9.7, 15.0 ± 13.0 and 9.8 ± 3.8, respectively.

Table 1 Demographics data

	Patients (n = 49)	Controls (n = 49)
Gender (men/women)	27/22	27/22
Age[a] (mean ± SD, years)	47.7 ± 13.0	47.5 ± 12.7
CAG (mean ± SD)	72.1 ± 4.2	–
Age at onset (mean ± SD, years)	37.5 ± 12.5	–
Duration (mean ± SD, years)	10.0 ± 4.7	–
SARA (mean ± SD)	14.7 ± 7.3	–
Patients with dystonia	19 (39%)	–
Clinical subtype (1/2/3/4)	14/23/11/1	–

[a]P value = 0.932, t test.

Image acquisition

All subjects underwent a detailed MRI protocol on a Philips 3 T scanner that included (i) T1 volumetric sequence – sagittal orientation, slice thickness of 1 mm, echo time (TE) = 3.2 ms, repetition time (TR) = 7.1 ms, excitation angle (flip angle) 8°, isotropic voxels of 1.0 × 1.0 × 1.0 mm^3, field-of-view (FOV) = 240 × 240 × 180; (ii) T2 sequence – coronal multi-echo (five echos) T2-weighted images with TE = 30 ms, TR = 3300 ms, voxels reconstructed to 0.42 × 0.42 × 3.00 mm^3, FOV = 180 × 180; (iii) FLAIR sequence – coronal and axial orientation, T2-weighted images anatomically aligned at the hippocampus with the gap between the slices 1 mm, TE = 140 ms, TR = 12 000 ms, time inversion = 2850 ms, voxels reconstructed to 0.45 × 0.45 × 4.00 mm^3, FOV = 220 × 206.

All images were first reviewed and those patients who had abnormalities unrelated to MJD/SCA3 (e.g. white matter disease, minor strokes) or significant motion artifacts were excluded. Then, T1 volumetric images were used for all further analyses in the FreeSurfer software.

Cortical thickness analyses

Cortical thickness was determined using the FreeSurfer software v.5.3. This measure was chosen because it is more sensitive to cortical variations than area and volume [13]. Measurements were performed according to the protocol suggested by Fischl and Dale [11].

Images were corrected for magnetic field inhomogeneity, aligned to the Talairach and Tournoux atlas [14] and skull-stripped. Next, voxels were labeled as gray matter, white matter or cerebrospinal fluid. From these, using triangle meshes, two surfaces were created: the white surface, which is the interface between gray matter and white matter, and the pial surface [11]. Cortical thickness was calculated as the shortest distance between the pial and white surface at each vertex across the cortical mantle. For all analyses, a Gaussian filter with 10 mm full width at half maximum was used for smoothing the surface. Furthermore, estimated total intracranial volume (eTIV) [15] and the volume for subcortical regions [16] were calculated. Regional cortical thickness variations between the patient and control groups were assessed using a general linear model (GLM) with age, gender and eTIV as covariates. Monte Carlo simulations were then employed to correct for multiple comparisons thus enabling the identification of significant vertex-wise group clusters. This analysis was performed using the Qdec suite which is part of the FreeSurfer toolbox (https://surfer.nmr.mgh.harvard.edu/fswiki/FsTutorial/QdecGroupAnalysis_freeview).

In addition to vertex-wise comparisons, FreeSurfer enables the comparison of cortical thickness and subcortical volume measurements for parcellation [16,17] taking into account anatomical atlases such as that proposed by Desikan *et al.* [18]. In this analysis, another GLM with age, gender and eTIV as covariates was performed to assess cortical thickness and subcortical volume differences between the two groups for each region. In order to correct for multiple comparisons, the Dunn–Sidak multiple comparison test (level of significance $a = 0.001$) was employed. This analysis was performed using the SYSTAT software v13.0 (San José, CA, USA).

Correlation analyses

Cortical data

For correlation analyses with clinical and genetic data, only those regions where cortical thickness was reduced in MJD/SCA3 patients were investigated. First, a simple regression was performed to investigate the association between cortical thickness of those regions and severity of disease (SARA score). Next, multiple regression analyses were performed to investigate (i) the determinants of cortical damage and (ii) possible correlations with neuropsychological data. In the former, age, age at onset, disease duration and length of the expanded CAG repeat were used as regressors. In the latter, BDI, BAI, SARA, age, gender and educational level were included as covariates in the model.

Systat v13.0 was employed for all these analyses. The P values were set to 0.0014 (Dunn–Sidak correction for multiple comparisons).

Subcortical data

Linear regression analyses to investigate possible relationships between subcortical volumes and severity of disease (SARA score) were used, adjusted for the variables eTIV and gender. These analyses were performed in SYSTAT v13.0 and the level of significance was set at $P = 0.003$ (corrected for multiple comparisons, Dunn–Sidak).

Results

Cortical thickness analyses

Using vertex-wise analysis, significant differences in cortical thickness between patients and controls were found in the left hemisphere at the superior frontal, superior temporal and precentral cortices, and in the

right hemisphere at the superior frontal cortex. These data are shown in Fig. 1 and Data S1.

Using the Desikan *et al*. atlas, significant cortical thinning was found in several regions of both hemispheres (Table 2).

Volumetric analyses

Several subcortical structures presented significantly smaller volumes in patients with MJD/SCA3 compared with healthy controls (Table 3). Interestingly, both hippocampi were also atrophic in the MJD/SCA3 group (right, 4026 ± 474 vs. 4435 ± 507 mm^3, $P < 0.001$; left, 3941 ± 482 vs. 4259 ± 489 mm^3, $P < 0.001$).

Correlation analyses

Cortical data

Single variable. In the group of patients with MJD/SCA3, the SARA scores showed a significant inverse correlation with cortical thickness of the left precentral gyrus ($r = -0.302$, $P = 0.035$), anterior transverse temporal gyrus ($r = -0.303$, $P = 0.034$), superior temporal sulcus ($r = -0.354$, $P = 0.013$), caudal middle frontal cortex ($r = -0.330$, $P = 0.020$), paracentral cortex ($r = -0.311$, $P = 0.03$) and transverse temporal cortex ($r = -0.346$, $P = 0.015$).

Multiple regression. In the multiple regression model, the thickness of the right angular gyrus, the posterior ramus of the left lateral sulcus and left caudal middle frontal cortex were significantly correlated with age, age at onset and disease duration (Table 4). No correlation between the length of the expanded CAG repeat and thickness measurements was found.

Regarding neuropsychological tests, a correlation was found between the similarity test (Wechsler Intelligence Adult scale III subtest) and precentral gyrus thickness; the Raven Progressive Matrix Test (General Scale) and middle occipital gyrus thickness; the similarity test and superior occipital gyrus thickness (Table 5).

Subcortical data. A significant correlation was found between SARA scores and subcortical volumes: brainstem ($r = 0.581$, $P < 0.001$), left thalamus volume ($r = 0.624$, $P < 0.001$) and ventral diencephalon both at right ($r = 0.575$, $P < 0.001$) and left ($r = 0.641$, $P < 0.001$) (Data S2). Duration of the disease also correlated with volumes of left ($r = 0.619$, $P < 0.001$) and right ($r = 0.578$, $P < 0.001$) ventral diencephalon and right cerebellar white matter ($r = 0.543$, $P = 0.001$) (Data S3). No correlations between subcortical volumes and age, age at onset and length of the expanded CAG repeat were found.

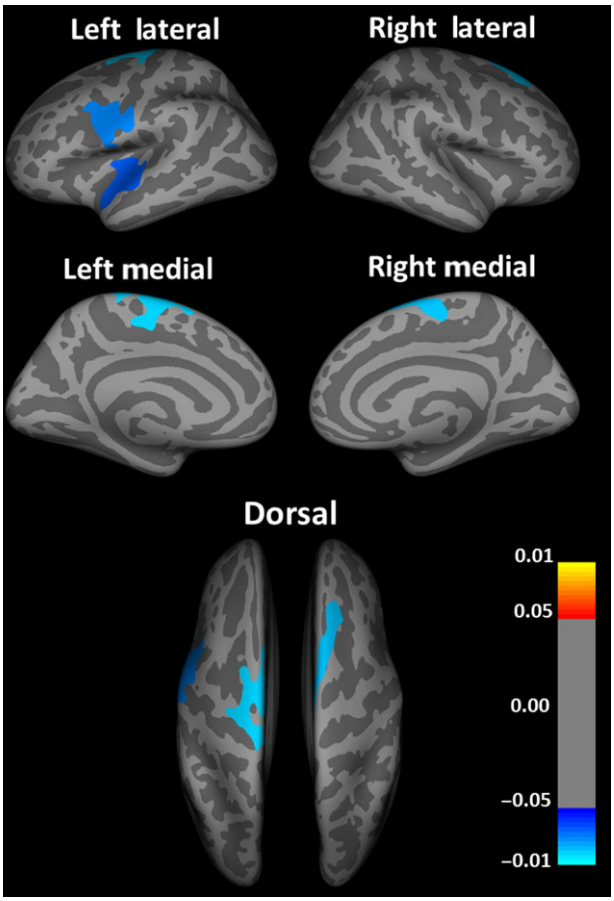

Figure 1 Map for group difference between patients and controls regarding cortical thickness; vertex-by-vertex analysis.

Discussion

This is the first study specifically devoted to investigating cerebral cortical damage in MJD/SCA3, using high resolution MRI scans and robust software for cortical thickness measurements (FreeSurfer). Multifocal cortical damage in the disease in a large cohort of patients was demonstrated. Motor regions of the frontal lobes were particularly affected, but cortical thinning also included areas of the parietal, temporal and occipital lobes. Gliosis and neuronal loss probably underlie these volumetric abnormalities [19]. Previous studies have indeed found loss of giant Betz neurons of layer V predominantly in the primary motor cortex of MJD/SCA3 patients, which is in line with our own results [20]. Although several atrophic cortical areas were found, damage was not homogeneously distributed over the cortical mantle. If it is considered that ataxin-3 (both normal and expanded) is expressed all over the cortex [21], this suggests that some neurons, such as pyramidal cells, are more vulnerable to the harmful effects of the mutant protein. These neurons

Table 2 Gyral-based areas with cortical thinning in patients with MJD/SCA3

Structure	MJD mean (mm)	Control mean (mm)
Left hemisphere		
Middle occipital gyrus	2.27 ± 0.19	2.40 ± 0.17
Precentral gyrus	2.49 ± 0.18	2.63 ± 0.20
Anterior transverse temporal gyrus	2.13 ± 0.27	2.31 ± 0.24
Posterior ramus of the lateral sulcus	2.14 ± 0.22	2.30 ± 0.20
Inferior part of the precentral sulcus	2.12 ± 0.15	2.26 ± 0.16
Superior temporal sulcus	2.19 ± 0.17	2.32 ± 0.14
Right hemisphere		
Paracentral lobule and sulcus	1.98 ± 0.18	2.16 ± 0.17
Middle-posterior part of the cingulate gyrus and sulcus	2.35 ± 0.19	2.47 ± 0.14
Short insular gyri	3.35 ± 0.30	3.49 ± 0.19
Superior occipital gyrus	1.89 ± 0.19	2.03 ± 0.21
Angular gyrus	2.35 ± 0.17	2.47 ± 0.17
Precentral gyrus	2.43 ± 0.25	2.62 ± 0.22
Posterior ramus of the lateral sulcus	2.22 ± 0.18	2.34 ± 0.14
Central sulcus	1.62 ± 0.12	1.72 ± 0.12
Marginal branch of the cingulate sulcus	1.99 ± 0.16	2.11 ± 0.16
Medial occipito-temporal sulcus and lingual sulcus	2.22 ± 0.21	2.37 ± 0.19

Table 3 Subcortical structures with volumetric reduction in patients with MJD/SCA3

Structure	MJD mean (mm^3)	Control mean (mm^3)
Left hemisphere		
Cerebellum WM	8511 ± 1951	15 204 ± 2298
Cerebellum GM	38 270 ± 4735	44 921 ± 6052
Thalamus	6184 ± 758	7439 ± 1036
Caudate	3005 ± 355	3471 ± 427
Putamen	5099 ± 608	5804 ± 956
Pallidum	1167 ± 200	1395 ± 261
Ventral diencephalon	2972 ± 364	3742 ± 374
Right hemisphere		
Cerebellum WM	8322 ± 1863	15 449 ± 2063
Cerebellum GM	38 781 ± 4895	45 603 ± 5819
Thalamus	5782 ± 640	6631 ± 737
Caudate	3169 ± 392	3678 ± 543
Putamen	5101 ± 585	5747 ± 821
Pallidum	1186 ± 163	1565 ± 240
Ventral diencephalon	3018 ± 352	3852 ± 460
Brainstem	14 313 ± 2367	20 929 ± 2445

WM, white matter; GM, gray matter.

with long projections have a high metabolic demand to support the transport of proteins and organelles all along the axon. Such metabolic needs might be compromised due to mutant ataxin-3 deleterious effects such as dysfunction of the ubiquitin-proteasome system and mitochondrial failure [22].

Most MRI-based studies in MJD/SCA3 focused on the cerebellum and subcortical structures [5,23]. In accordance with these previous reports, our data also indicate volumetric reduction of both thalami and basal ganglia, as well as the cerebellum and brainstem. These are regions involved in motor control that account for the main clinical manifestations found in patients with MJD/SCA3, such as ataxia, dystonia and pyramidal signs. In our analyses, severity of ataxia correlated with brainstem and thalamic volumes, which gives further support to this hypothesis. On the other hand, available data that report cortical damage in MJD/SCA3 are scant [5]. Some PET and SPECT studies identified cortical areas of hypoperfusion in SCA3, including the inferior and superior portions of the frontal lobes, lateral portion of the temporal lobes, parietal lobes and occipital lobes [8]. D'Abreu *et al.* [7] performed VBM analyses and found widespread cortical atrophy in a large cohort of patients. In another study, Goel *et al.* [24] found cortical thinning in the superior temporal gyrus and inferior frontal gyrus in both hemispheres. These results are similar to those reported here, but atrophy in some regions reported in that paper, such as the insula, cuneus and precuneus, were not found [7]. This apparent discrepancy is probably explained by the different technical approaches employed by VBM and FreeSurfer to determine gray matter volumes. Briefly, VBM merges information about morphology, size and position of the cortex to determine gray matter densities. In contrast, FreeSurfer performs an automated segmentation and calculates thickness in native space images using a surface-based model, measuring differences in gray matter based on the geometry of the cortical surface [11,16,17,25–29]. Therefore, cortical thickness is a direct measure and less susceptible to errors induced by positional variance, since the cortex extraction follows the gray matter surface [30,31]. Studies that attempted to compare both methods found that surface-based techniques are more sensitive to detect cerebral cortex abnormalities compared with VBM, both in normal aging [13] and in neuropsychiatric disorders [25,32,33].

In SCA3, some clinical features are mostly determined by expanded CAG repeat length, such as dystonia, whereas others are time-dependent, such as peripheral nerve damage [34]. Therefore, the determinants of cortical damage were identified using multiple variable regression analyses. The thickness of the right angular gyrus, caudal middle frontal cortex and posterior fissure significantly correlated with disease duration but not with CAG repeat length. These results

Table 4 Multiple regression of thickness measurements versus clinical parameters in the MJD/SCA3 group

Structure	*R* adjusted	*P*-valor regression	Independent variables	Regression coefficient	*P* value
LH_ Caudal middle frontal cortex	0.569	0.004	*Age*	−0.240	0.029
			CAG	−0.007	0.129
			Onset	0.239	0.029
			Duration	0.223	0.040
			Gender	0.070	0.105
RH_Angular gyrus	0.662	< 0.001	*Age*	−0.390	0.001
			CAG	−0.003	0.469
			Onset	0.386	0.001
			Duration	0.376	0.001
			Gender	0.111	0.010
RH_ Posterior ramus of the lateral sulcus	0.603	0.001	*Age*	−0.266	0.029
			CAG	−0.006	0.232
			Onset	0.258	0.033
			Duration	0.248	0.039
			Gender	0.058	0.219

Table 5 Multiple regression of thickness measurements versus neuropsychological tests in the MJD/SCA3 group

Neuropsychological test	*R* adjusted	*P* value adjusted	Independent variables	Regression coefficient	*P* value
Similarity[a]	0.823	0.001	LH_Precentral gyrus	**−13.261**	**0.041**
			BDI	−0.260	0.044
			BAI	0.217	0.156
			SARA	0.160	0.395
			Age	0.057	0.611
			Educational level	1.543	< 0.001
			Gender	−3.319	0.164
RAVEN[b]	0.900	< 0.001	LH_Middle occipital gyrus	**−16.528**	**0.025**
			BDI	−0.209	0.131
			BAI	0.135	0.419
			SARA	−0.047	0.805
			Age	−0.170	0.171
			Educational level	2.708	< 0.001
			Gender	0.497	0.846
Similarity[a]	0.837	< 0.001	RH_ Superior occipital gyrus	**−20.066**	**0.017**
			BDI	−0.251	0.044
			BAI	0.151	0.315
			SARA	0.191	0.278
			Age	0.018	0.872
			Educational level	1.688	< 0.001
			Gender	−2.611	0.255

[a]Similarity: Wechsler Intelligence Adult scale III subtest; [b]RAVEN: Raven Progressive Matrix Test (General Scale).

suggest that cerebral cortical damage in MJD/SCA3 is mostly time-dependent, rather than CAG expansion-dependent. It seems that the MJD/SCA3 mutation accelerates an age-dependent phenomenon of neuronal death in some cortical regions.

A major finding in our analyses was motor cortex atrophy in MJD/SCA3 compared with healthy controls. Furthermore, severity of disease, expressed by SARA scores, correlated with thickness of precentral and paracentral cortices. Taken together, these data indicate that motor impairment in MJD/SCA3 not only is caused by cerebellar damage but is also related to cerebral cortex atrophy. A possible explanation is that precentral neuronal loss might disrupt the corticospinal, cortico-bulbar and cortico-ponto-cerebellar tracts. This hypothesis is supported by two recently published diffusion tensor imaging-based studies in MJD/SCA3, which found abnormal radial diffusivity in the frontal lobe white matter [4]. It would be interesting now to validate these findings in a longitudinal study and to separately evaluate patients with different clinical subtypes of the disease.

Several papers have described cognitive impairment in patients with MJD/SCA3, including verbal and visual memory deficits, visuospatial dysfunction and executive dysfunction [9]. Depressive symptoms are common as well [9]. Some authors consider that these neuropsychological abnormalities in MJD/SCA3 are related to the cerebellar cognitive affective syndrome (CCAS) [35]. This syndrome was first described by Schmahmann and Sherman [36] in patients presenting behavioral changes and multiple cognitive deficits due to lesions confined within the cerebellum. The anatomical substrate for CCAS probably involves dysfunction of circuits that connect the cerebellum with the prefrontal, superior parietal, superior temporal and limbic cortices [36]. Although this is a sound hypothesis, one must consider that patients with MJD/SCA3 have extra-cerebellar pathology. In fact, volumetric reduction in some cortical areas that might be involved with the mental abnormalities found in MJD/SCA3 has been found. Occipital and cingulate gyri damage, for instance, may be associated with visuospatial deficits and mood disorders, respectively. Bilateral hippocampal atrophy was also found in the MJD/SCA3 group, which may help to explain both visual and verbal memory impairment in these patients. In addition, some of the affected cortical regions correlated with neuropsychological tests, which further supports the concept that cognitive impairment and cerebral damage are related in MJD/SCA3. The thickness of the right superior occipital gyrus presented a direct correlation with the similarity subscore of the Wechsler Intelligence Adult scale III and the left middle occipital gyrus also correlated with the Raven Progressive Matrix Test (General Scale). These findings can be explained because these subtests require the individual to describe how alike two given things are (similarity) as well as to perform a mental visualization of the patterns used in the Raven progressive matrix, thus demanding intact visuospatial functioning. In a recent study, Zamboni *et al.* performed a functional MRI study using a visuospatial task (similar to the similarity test) in a cohort of healthy elderly and looked for the neuroanatomical correlates for this cognitive function. Interestingly, they found the superior occipital cortices to be significantly activated, which supports the concept that it is an important structure for recognition and visual-based memory retrieval [37]. An unexpected finding was the association between left precentral gyrus thickness and similarity subscore. However, Porro *et al.* [38] in a functional MRI study found activation of this region in cognitive tasks that involve motor imagery.

Conclusion

Patients with MJD/SCA3 have cerebral cortical damage, including regions associated with motor and cognitive function. Interestingly, motor and cognitive dysfunction in these patients was significantly associated with the volumetric reduction of some cortical regions. Furthermore, cerebral cortical damage in MJD/SCA3 is mostly time-dependent rather than (CAG) expansion-dependent. Taken together, these data indicate that neurodegeneration in MJD/SCA3 extends far beyond the cerebellum and that some clinical manifestations may be caused by direct cerebral cortical damage.

Acknowledgements

This work was supported by Fundacão de Amparo à Pesquisa do Estado de São Paulo (FAPESP), Coordenacão de Aperfeicoamento de Pessoal de Nível Superior (CAPES) and Conselho Nacional de Desenvolvimento Científico e Tecnológico (CNPq).

Disclosure of conflicts of interest

The authors declare no financial or other conflicts of interest.

Supporting Information

Additional Supporting Information may be found in the online version of this article:

Data S1. Cortical regions with significant thickness differences between patients and controls.
Data S2. Multiple regression of subcortical volume measurements versus SARA score corrected to eTIV and gender in the MJD/SCA3 group.
Data S3. Multiple regression of subcortical volume measurements versus duration score corrected to eTIV and gender in the MJD/SCA3 group.

References

1. D'Abreu A, França MC Jr, Paulson HL, Lopes-Cendes I. Caring for Machado–Joseph disease: current understanding and how to help patients. *Parkinsonism Relat Disord* 2010; **16:** 2–7.
2. D'Abreu A, França MC Jr, Yasuda CL, Souza MS, Lopes-Cendes I, Cendes F. Thalamic volume and dystonia in Machado–Joseph disease. *J Neuroimaging* 2011; **21:** 91–93.
3. Schulz JB, Borkert J, Wolf S, *et al*. Visualization, quantification and correlation of brain atrophy with clinical symptoms in spinocerebellar ataxia types 1, 3 and 6. *Neuroimage* 2010; **49:** 158–168.
4. Guimaraes RP, D'Abreu A, Yasuda CL, *et al*. A multimodal evaluation of microstructural white matter damage in spinocerebellar ataxia type 3. *Mov Disord* 2013; **28:** 1125–1132.
5. Tokumaru AM, Kamakura K, Maki T, *et al*. Magnetic resonance imaging findings of Machado–Joseph disease: histopathologic correlation. *J Comput Assist Tomogr* 2003; **27:** 241–248.
6. Rub U, Brunt ER, Deller T. New insights into the pathoanatomy of spinocerebellar ataxia type 3 (Machado–Joseph disease). *Curr Opin Neurol* 2008; **21:** 111–116.
7. D'Abreu A, França MC Jr, Yasuda CL, Campos BA, Lopes-Cendes I, Cendes F. Neocortical atrophy in Machado–Joseph disease: a longitudinal neuroimaging study. *J Neuroimaging* 2012; **22:** 285–291.
8. Etchebehere EC, Cendes F, Lopes-Cendes I, Pereira JA, Lima MC, Sansana CR, *et al*. Brain single-photon emission computed tomography and magnetic resonance imaging in Machado–Joseph disease. *Arch Neurol* 2001; **58:** 1257–1263.
9. Lopes TM, D'Abreu A, França MC Jr, *et al*. Widespread neuronal damage and cognitive dysfunction in spinocerebellar ataxia type 3. *J Neurol* 2013; **260:** 2370–2379.
10. Kawai Y, Takeda A, Abe Y, Washimi Y, Tanaka F, Sobue G. Cognitive impairments in Machado–Joseph disease. *Arch Neurol* 2004; **61:** 1757–1760.
11. Fischl B, Dale AM. Measuring the thickness of the human cerebral cortex from magnetic resonance images. *Proc Natl Acad Sci USA* 2000; **97:** 11050–11055.
12. Schmitz-Hubsch T, du Montcel ST, Baliko L, *et al*. Scale for the assessment and rating of ataxia: development of a new clinical scale. *Neurology* 2006; **66:** 1717–1720.
13. Hutton C, Draganski B, Ashburner J, Weiskopf N. A comparison between voxel-based cortical thickness and voxel-based morphometry in normal aging. *Neuroimage* 2009; **48:** 371–380.
14. Talairach J, Tournoux P. *Co-planar Stereotaxic Atlas of the Human Brain*. New York: Thieme, 1988.
15. Buckner RL, Head D, Parker J, *et al*. A unified approach for morphometric and functional data analysis in young, old, and demented adults using automated atlas-based head size normalization: reliability and validation against manual measurement of total intracranial volume. *Neuroimage* 2004; **23:** 724–738.
16. Fischl B, Salat DH, Busa E, *et al*. Whole brain segmentation: automated labeling of neuroanatomical structures in the human brain. *Neuron* 2002; **33:** 341–355.
17. Fischl B, van der Kouwe A, Destrieux C, *et al*. Automatically parcellating the human cerebral cortex. *Cereb Cortex* 2004; **14:** 11–22.
18. Desikan RS, Segonne F, Fischl B, *et al*. An automated labeling system for subdividing the human cerebral cortex on MRI scans into gyral based regions of interest. *Neuroimage* 2006; **31:** 968–980.
19. Durr A, Stevanin G, Cancel G, *et al*. Spinocerebellar ataxia 3 and Machado–Joseph disease: clinical, molecular, and neuropathological features. *Ann Neurol* 1996; **39:** 490–499.
20. Seidel K, Siswanto S, Brunt ER, den Dunnen W, Korf HW, Rub U. Brain pathology of spinocerebellar ataxias. *Acta Neuropathol* 2012; **124:** 1–21.
21. Paulson HL, Das SS, Crino PB, *et al*. Machado–Joseph disease gene product is a cytoplasmic protein widely expressed in brain. *Ann Neurol* 1997; **41:** 453–462.
22. Costa MC, Paulson HL. Toward understanding Machado–Joseph disease. *Prog Neurobiol* 2012; **97:** 239–257.
23. Rub U, Gierga K, Brunt ER, *et al*. Spinocerebellar ataxias types 2 and 3: degeneration of the pre-cerebellar nuclei isolates the three phylogenetically defined regions of the cerebellum. *J Neural Transm* 2005; **112:** 1523–1545.
24. Goel G, Pal PK, Ravishankar S, *et al*. Gray matter volume deficits in spinocerebellar ataxia: an optimized voxel based morphometric study. *Parkinsonism Relat Disord* 2011; **17:** 521–527.
25. Park H-J, Lee JD, Kim EY, *et al*. Morphological alterations in the congenital blind based on the analysis of cortical thickness and surface area. *Neuroimage* 2009; **47:** 98–106.
26. Ashburner J. Computational anatomy with the SPM software. *Magn Res Imaging* 2009; **27:** 1163–1174.
27. Ashburner J, Friston KJ. Voxel-based morphometry – the methods. *Neuroimage* 2000; **11:** 805–821.
28. Dale AM, Fischl B, Sereno MI. Cortical surface-based analysis. I. Segmentation and surface reconstruction. *Neuroimage* 1999; **9:** 179–194.
29. Fischl B, Sereno MI, Dale AM. Cortical surface-based analysis. II: Inflation, flattening, and a surface-based coordinate system. *Neuroimage* 1999; **9:** 195–207.
30. MacDonald D, Kabani N, Avis D, Evans AC. Automated 3-D extraction of inner and outer surfaces of cerebral cortex from MRI. *Neuroimage* 2000; **12:** 340–356.
31. Kim JS, Singh V, Lee JK, *et al*. Automated 3-D extraction and evaluation of the inner and outer cortical surfaces using a Laplacian map and partial volume effect classification. *Neuroimage* 2005; **27:** 210–211.
32. Pereira JB, Ibarretxe-Bilbao N, Marti MJ, *et al*. Assessment of cortical degeneration in patients with Parkinson's disease by voxel-based morphometry, cortical folding, and cortical thickness. *Hum Brain Mapp* 2012; **33:** 2521–2534.
33. Voets NL, Hough MG, Douaud G, *et al*. Evidence for abnormalities of cortical development in adolescent-onset schizophrenia. *Neuroimage* 2008; **43:** 665–675.
34. Schmitz-Hübsch T, Coudert M, Bauer P, *et al*. Spinocerebellar ataxia types 1, 2, 3, and 6: disease severity and nonataxia symptoms. *Neurology* 2008; **71:** 982–989.
35. Braga-Neto P, Dutra LA, Pedroso JL, *et al*. Cognitive deficits in Machado–Joseph disease correlate with hypoperfusion of visual system areas. *Cerebellum* 2012; **11:** 1037–1044.

36. Schmahmann JD, Sherman JC. The cerebellar cognitive affective syndrome. *Brain* 1998; **121:** 561–579.
37. Zamboni G, de Jager CA, Drazich E, *et al*. Structural and functional bases of visuospatial associative memory in older adults. *Neurobiol Aging* 2013; **34:** 961–972.
38. Porro CA, Francescato MP, Cettolo V, *et al*. Primary motor and sensory cortex activation during motor performance and motor imagery: a functional magnetic resonance imaging study. *J Neurosci* 1996; **16:** 7688–7698.